The Kinetic and Physical Basis of K_{ATP} Channel Gating: Toward a Unified Molecular Understanding

D. Enkvetchakul,* G. Loussouarn,[†] E. Makhina,[†] S. L. Shyng,[†] and C. G. Nichols[†]

*Division of Renal Medicine and [†]Department of Cell Biology and Physiology, Washington University School of Medicine, St. Louis, Missouri 63110 USA

ABSTRACT　K_{ATP} channels can be formed from Kir6.2 subunits with or without SUR1. The open-state stability of K_{ATP} channels can be increased or reduced by mutations throughout the Kir6.2 subunit, and is increased by application of PIP_2 to the cytoplasmic membrane. Increase of open-state stability is manifested as an increase in the channel open probability in the absence of ATP (Po_{zero}) and a correlated decrease in sensitivity to inhibition by ATP. Single channel lifetime analyses were performed on wild-type and I154C mutant channels expressed with, and without, SUR1. Channel kinetics include a single, invariant, open duration; an invariant, brief, closed duration; and longer closed events consisting of a "mixture of exponentials," which are prolonged in ATP and shortened after PIP_2 treatment. The steady-state and kinetic data cannot be accounted for by assuming that ATP binds to the channel and causes a gate to close. Rather, we show that they can be explained by models that assume the following regarding the gating behavior: 1) the channel undergoes ATP-insensitive transitions from the open state to a short closed state (C_f) and to a longer-lived closed state (C_0); 2) the C_0 state is destabilized in the presence of SUR1; and 3) ATP can access this C_0 state, stabilizing it and thereby inhibiting macroscopic currents. The effect of PIP_2 and mutations that stabilize the open state is then to shift the equilibrium of the "critical transition" from the open state to the ATP-accessible C_0 state toward the O state, reducing accessibility of the C_0 state, and hence reducing ATP sensitivity.

INTRODUCTION

ATP-sensitive potassium (K_{ATP}) channels are inhibited by intracellular ATP and thus couple cellular metabolism to membrane potential (Ashcroft, 1988; Nichols and Lederer, 1991). Structurally unique among potassium channels, they are normally formed from an ATP-binding-cassette protein (sulfonylurea receptor, SURx) and an inward rectifier (Kir6.x) subunit (Aguilar-Bryan et al., 1995; Inagaki et al., 1995, 1996) with a 4:4 stoichiometry (Shyng and Nichols, 1997; Clement et al., 1997; Inagaki et al., 1997). The SURx subunit confers sensitivity of the channel to sulfonylureas, MgADP, and potassium channel openers (Nichols et al., 1996; Gribble et al., 1997; Shyng et al., 1997b). Multiple structure-function analyses demonstrate that the Kir6.x subunit forms the pore and controls the hallmark inhibition by ATP (Shyng et al., 1997a; Tucker et al., 1997, 1998; Drain et al., 1998). However, the mechanism of this inhibition remains unclear.

Recent reports indicate that membrane-bound phospholipids bind to various inward rectifier K^+ channels, stabilizing them in an active conformation (Hilgemann and Ball, 1996; Fan and Makielski, 1997; Huang et al., 1998) and K_{ATP} channels are no exception in being activated by PIP_2 (Fan and Makielski, 1997; Hilgemann and Ball, 1996). In controlling K^+ channel activation, the more negatively charged the phospholipid, the more potent is the activating effect (Hilgemann and Ball, 1996; Fan and Makielski, 1997). The inhibitory effect of intracellular nucleotides on K_{ATP} channels also depends on the number of phosphate groups in the molecule (Ashcroft, 1988; Lederer and Nichols, 1989), which might suggest that PIP_2 activation and ATP inhibition are related phenomena. Consistent with this hypothesis, PIP_2 has a profound effect on the sensitivity of SUR1+Kir6.2 channels to ATP inhibition (Shyng and Nichols, 1998; Baukrowitz et al., 1998). In the present study we have further examined the interaction of PIP_2 and Kir6.2 subunits. The results demonstrate that PIP_2-induced channel activation and desensitization to ATP is also observed for channels formed from Kir6.2 subunits alone (Tucker et al., 1997; Baukrowitz et al., 1998), but with altered quantitative responses. Both PIP_2 and multiple mutations of the Kir6.2 channel pore region affect the intrinsic stability of the channel open state and the apparent affinity for ATP (Shyng et al., 1997a; Tucker et al., 1998; Trapp et al., 1998; Drain et al., 1998). These findings indicate that, rather than causing closure of the K_{ATP} channel, the inhibitory action of ATP is to stabilize a closed state. Consideration of these constraints suggests kinetic models that can account both for the behavior of K_{ATP} channels formed from Kir6.2 subunits with or without SUR1, and the action of PIP_2 on the channels.

METHODS

Molecular biology

Point mutations were prepared by overlap extension at the junctions of the relevant residues by sequential polymerase chain reaction (PCR). Resulting PCR products were subcloned into pECE or pCMV6b vectors and sequenced to verify the correct mutant construct, before transfection.

A

I154C[ΔC] + SUR

ATP 5 mM

0.5 mM

0 pA

-20 pA

30 secs

B

L157C[ΔC] + SUR

ATP 1 mM

10 mM

0 pA

-16 pA

30 secs

C

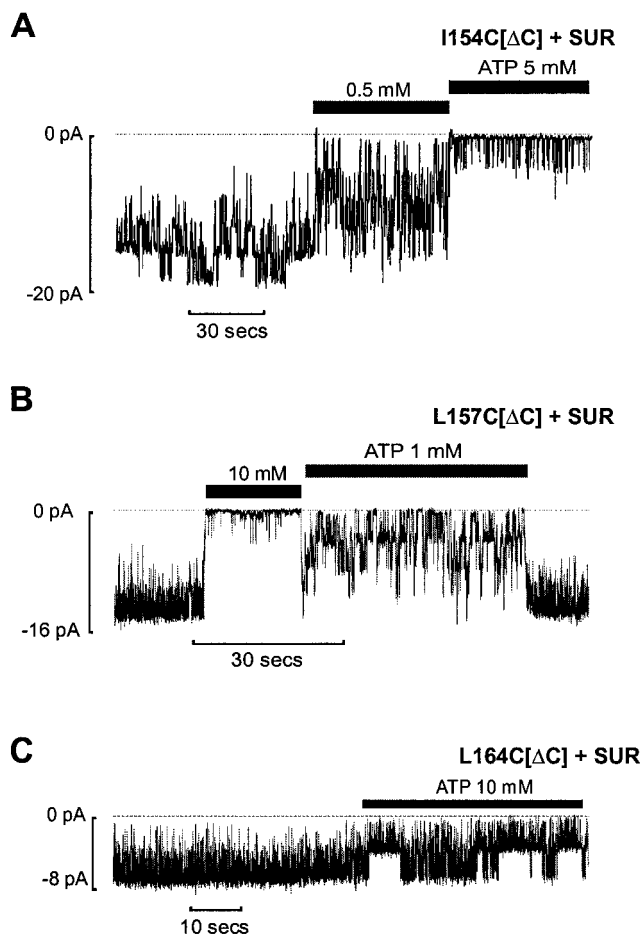**L164C[ΔC] + SUR**

ATP 10 mM

0 pA

-8 pA

10 secs

FIGURE 1 M2 cysteine mutations can generate very ATP-insensitive channels with very high open probability. Representative currents recorded from inside-out membrane patches containing only a few (A) I154C[ΔC] + SUR1, (B) L157C[ΔC] + SUR1, or (C) L164C[ΔC] + SUR1 mutant K$_{ATP}$ channels at −50 mV in K-INT solution (see Methods). Patches were exposed to differing [ATP] as indicated

Expression of K$_{ATP}$ channels in COSm6 cells

COSm6 cells were plated at a density of ~2.5 × 10^5 cells per well (30 mm six-well dishes) and cultured in Dulbecco's Modified Eagle Medium plus 10 mM glucose (DMEM-HG), supplemented with fetal calf serum (FCS, 10%). The next day, cells were transfected by incubation for 4 h at 37°C in DMEM containing 10% Nuserum, 0.4 mg/ml diethylaminoethyl-dextran, 100 μM chloroquine, and 5 μg each of pCMV6b-Kir6.2, pECE-SUR1, and pECE-GFP (green fluorescent protein) cDNA. Cells were subsequently incubated for 2 min in phosphate-buffered salt solution containing DMSO (10%), and returned to DMEM-HG plus 10% FCS.

Patch-clamp measurements

K$_{ATP}$ currents were assayed using patch-clamp measurements 2–4 days after transfection. Experiments were made at room temperature, in an oil-gate chamber which allowed the solution bathing the exposed surface of the isolated patch to be changed in 50 ms. Micropipettes were pulled from thin-walled glass (WPI Inc., New Haven, CT) on a horizontal puller (Sutter Instrument, Co., Novato, CA). Electrode resistance was typically 0.5–1 MΩ (5–10 MΩ for single channel currents) when filled with K-INT

solution (see below). Microelectrodes were "sealed" onto cells that fluoresced green under UV illumination, by applying light suction to the rear of the pipette. Inside-out patches were obtained by lifting the electrode and then passing the electrode tip through the oil-gate. Membrane patches were voltage-clamped with an Axopatch 1D or 200A patch-clamp (Axon Inc., Foster City, CA). The standard bath (intracellular) and pipette (extracellular) solution used in these experiments (K-INT) had the following composition: 140 mM KCl, 10 mM K-HEPES, 1 mM K-EGTA, pH 7.3. PIP2 was bath sonicated in ice for 30 min before use. All currents were measured at a membrane potential of −50 mV (pipette voltage = +50 mV). Data were normally filtered at 0.5–20 kHz, signals were digitized at 22 or 88 kHz (Neurocorder, Neurodata, NY) and stored on video tape. Experiments were replayed onto a chart recorder, or digitized into a microcomputer using Axotape or Fetchex software (Axon Inc.). Off-line analysis was performed using Fetchan, pSTAT, and Microsoft Excel programs. The threshold for judging the open state was set at half the single channel amplitude. Wherever possible, data are presented as mean ± SE. (standard error of the mean). Microsoft Solver was used to fit data by a least-square algorithm.

Model simulations

Probability density functions of kinetic models were calculated with Mathcad software (MathSoft, Inc., Cambridge, MA) using matrix mathematics as described by Colquhoun and Hawkes (1977, 1981, 1995). The probability density function of a set of states A with k states is given by:

$$f(t) = \Phi\exp(t^*Q_{AA})(-Q_{AA})u_A. \tag{1}$$

Table 1 K$_{1/2,ATP}$ and Po$_{zero}$ values (estimated from noise analysis or single channels) for mutant Kir6.2 + SUR1 channels examined in this study (L164, R176 mutants), in Shyng et al. (1997a, N160 mutants) and in Loussouarn et al. (2000, Cysteine substitutions)

	Po$_{zero}$ ± SE	mean K$_{1/2,ATP}$ (μM) ± SE
WT	0.45 ± 0.09	12 ± 1.6
L164T	0.89 ± 0.01	4,300
L164G	0.89 ± 0.03	3,600
L164A	0.87 ± 0.02	520
L164V	0.78 ± 0.04	7
R176A	0.01 ± 0.001	5
N160D	0.83 ± 0.01	46
N160A	0.76 ± 0.02	6
N160E	0.83 ± 0.03	18
Ctrl	0.88 ± 0.02	1,060 ± 10
Ctrl N/D	0.88 ± 0.01	1,060 ± 24
Ctrl-N153C	0.88 ± 0.02	230 ± 76
Ctrl-I154C	0.89 ± 0.01	330 ± 30
Ctrl-L157C N/D	0.89 ± 0.01	420 ± 270
Ctrl-M158C N/D	0.89 ± 0.02	4,200 ± 1300
Ctrl-A161C N/D	0.88 ± 0.01	110 ± 8
Ctrl-I162C N/D	0.86 ± 0.03	33 ± 6
Ctrl-M163C N/D	0.90 ± 0.02	190 ± 54
Ctrl-L164C N/D	0.89 ± 0.01	>100,000
Ctrl-I167C N/D	0.88 ± 0.02	1,100 ± 250
Ctrl-M169C N/D	0.90 ± 0.01	110 ± 17
Ctrl-T171C	0.91 ± 0.02	2,800 ± 820
Ctrl-Q173C	0.88 ± 0.01	33 ± 4
Ctrl-H175C N/D	0.90 ± 0.03	24,500 ± 4970

All channels were coexpressed with SUR1 subunits. WT refers to wild-type Kir6.2 construct. Ctrl refers to Kir6.2[C166S, ΔC36] background, with or without additional N160D mutation (N/D), or with cysteine (C) substitutions as indicated.
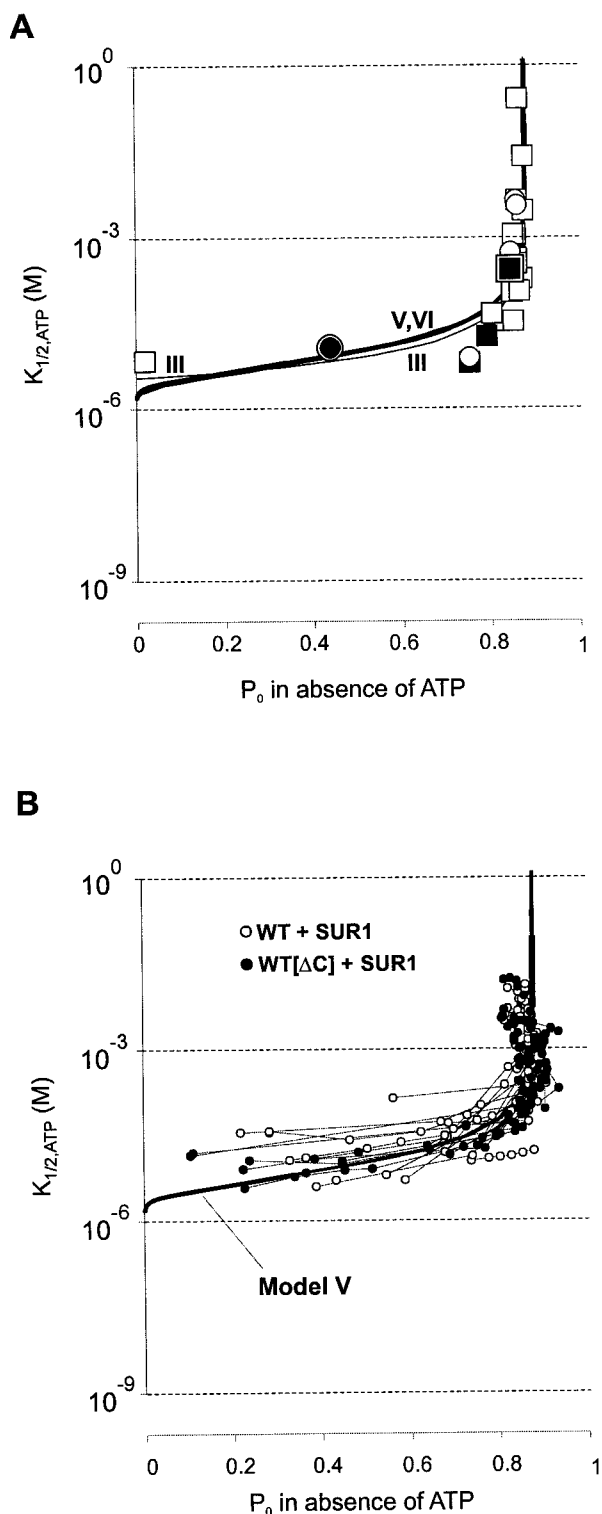
A

B

○ WT + SUR1
● WT[ΔC] + SUR1

Model V

FIGURE 2 $K_{1/2,ATP}$ versus Po_{zero} for coexpressed Kir6.2 + SUR1 channels (data summarized with errors in Table 1). (*A*) Large symbols represent mean values for different Kir6.2 mutant constructs (*open squares:* cysteine substitutes on ΔC36,C166S background, Loussouarn et al., 2000, and R176A, Shyng and Nichols, 1998; *closed squares:* N160x mutations, Shyng et al., 1997a; *open circles:* L164x mutants; *double circle:* wild-type Kir6.2; *double square:* I154C[ΔC]). Superimposed smooth lines correspond to predictions of Models III, V, and VI as indicated, with continuous

where Q_{AA} is a submatrix of Q and is based on rate constants, Φ, a 1 x k row vector containing the probabilities of starting in each of the states *A* at time 0, and u_A is a k × 1 column vector whose elements are all 1. The expression "$\exp(t^*Q_{AA})$" was calculated using the spectral expansion of Q_{AA}.

RESULTS

Multiple M2 mutations desensitize the channel to ATP and stabilize the channel open state

Recent evidence suggests that ATP may act by stabilizing a closed state of the channel because changes in open probability in zero ATP correlate with changes in apparent ATP sensitivity (Shyng et al., 1997a, Trapp et al., 1998; Koster et al., 1999; Shyng and Nichols, 1998). In particular, systematic mutations of residues in the M2 region of Kir6.2 cause wide variation of ATP sensitivity (Loussouarn et al., 2000). Three such mutations shown in Fig. 1 generate channels that are very insensitive to ATP, and have a very high open probability in the absence of ATP (typically 0.8–0.9), with the channels being in a nearly continuously "bursting" state. We estimated ATP sensitivity and Po_{zero} (channel open probability in the absence of ATP) from experiments like those in Fig. 1 from amplitude histograms, or by noise analysis of patches containing a large number of channels. Table 1 and Fig. 2 *A* summarize the Po_{zero} and $K_{1/2,ATP}$ estimates for each of the M2 mutant channels coexpressed with SUR1. Although comparison of Po_{zero}-$K_{1/2,ATP}$ relationships between isolated mutations is not particularly informative, it is quite clear from the whole data set (Fig. 2 *A*), that Po_{zero} and $K_{1/2,ATP}$ are correlated, i.e., ATP sensitivity depends on the open-state stability.

The effect of PIP$_2$ on ATP sensitivity and open probability of K$_{ATP}$ channels formed of Kir6.2 subunits with or without SUR1

We have concentrated further analysis on wild-type Kir6.2 (full length: WT, or C-terminally truncated: WT[ΔC]) subunits, and on the high open-state stability mutant Kir6.2[I154C,ΔC] subunits (I154C[ΔC]). We previously demonstrated that PIP$_2$ increases Po_{zero} and $K_{1/2,ATP}$ of wild-type K$_{ATP}$ channels coexpressed with SUR1 (Shyng and Nichols, 1998). Fig. 3 shows representative recordings of currents generated by expression of WT[ΔC] and I154C[ΔC] subunits with (*A*), or without SUR1 (*B, C*). In each case, application of PIP$_2$ leads to an increase of open probability and to a decrease of ATP sensitivity (Shyng and Nichols, 1998; Baukrowitz et al., 1998). For WT, or

variation of K_{CO} (see text). (*B*) Small symbols represent individual patches from Kir6.2 (WT) + SUR1 (*closed symbols*, from Shyng and Nichols, 1998) or Kir6.2[ΔC25] (WT[ΔC]) + SUR1 (*open symbols*), before, and with time after, exposure to PIP$_2$. Individual patches are connected by thin lines. The heavy line represents predicted Po_{zero} versus $K_{1/2,ATP}$ relationship calculated from Model V (see text).
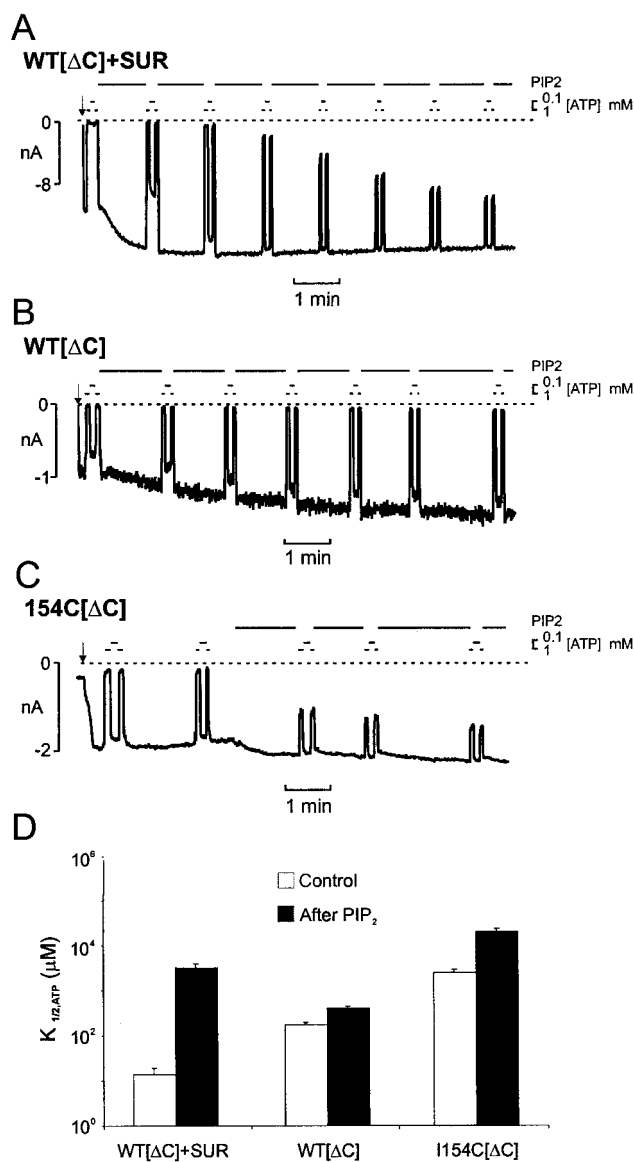
FIGURE 3 PIP_2 stimulates, and relieves ATP inhibition of, WT[ΔC] and I154C[ΔC] currents, with and without SUR1 coexpression. (*A–C*) Representative currents recorded from inside-out membrane patches containing WT[ΔC] subunits with (*A*), or without (*B*) SUR1, or I154C[ΔC] subunits without SUR1 (*C*). Currents were recorded at −50 mV in K-INT solution (see Methods). Patches were exposed to differing [ATP] or 5 μg/ml PIP_2 as indicated. (*D*) Mean $K_{1/2,ATP}$ for Kir6.2[ΔC25] channels expressed with or without SUR1, and Kir6.2[ΔC25, I154C] without SUR1, before and after 5–12 min treatment with 5 μg/ml PIP_2 (mean ± SE, *n* = 5–7 in each case).

WT[ΔC] channels co-expressed with SUR1, the time course of channel activation by PIP_2 is variable from patch to patch, and individual patches have quite variable open probability upon first isolation. Nevertheless, when the Po_{zero}-$K_{1/2,ATP}$ relationship is plotted, the trajectory, after application of PIP_2, is consistent from patch to patch and, moreover, follows the same trajectory as the relationship that is observed for multiple M2 mutations under ambient conditions after patch excision (Fig. 2 *B*).

WT[ΔC] channels have a higher $K_{1/2,ATP}$, but lower Po_{zero}, in the absence of SUR1 than in its presence (Fig. 4 *A*, Table 2; Tucker et al., 1997; Koster et al., 1999; Trapp et al., 1998), such that the absence of SUR1 does not simply shift the channels to a different position along the same $K_{1/2,ATP}$-Po_{zero} relationship. Table 2 and Fig. 4 *A* combine multiple data from the present study, as well as from Trapp et al. (1998) and Tucker et al. (1998) to show that M2 mutations expressed without SUR1 do nevertheless lie on a single $K_{1/2,ATP}$-Po_{zero} relationship (Fig. 4 *A*), but one that is shifted from that observed for SUR-coexpressed constructs (Fig. 2). Also, as shown in Fig. 3, 5 μg/ml PIP_2 does not affect the ATP sensitivity of WT[ΔC] without SUR1 channels to nearly the same degree as WT[ΔC]+SUR1 channels; the Po_{zero} does not rise to saturating levels, and there is only ~3-fold increase in $K_{1/2,ATP}$. However, for I154C[ΔC] channels, which have a higher intrinsic open-state stability (i.e., they are operating on the steeper part of the $K_{1/2,ATP}$-Po_{zero} relationship), stimulation by PIP_2 does lead to a rapid saturation of open probability (~0.9), and then a significant loss of ATP sensitivity (Fig. 3 *D*), $K_{1/2,ATP}$ increasing from 2.8 ± 0.6 mM to 18.3 ± 6.0 mM after 11 ± 3 min treatment with PIP_2 (*n* = 3, Figs. 3 and 4 *B*, *open small circles*).

Single channel analyses of WT and I154C channels expressed with and without SUR1 subunit

We have measured single channel currents from cells expressing WT subunits in the absence (Fig. 5 *A*) and presence (Figs. 5 *B*, 6) of SUR1. Figs. 5–7 also show Sigworth-Sine (Sigworth and Sine, 1987) representations of closed- and open-time histograms obtained from these recordings, after Gaussian filtering at 3–4 kHz (see Note 1 at end of text). As shown in numerous previous studies, wild-type (WT+SUR1) channel activity occurs in bursts. Single exponential functions would adequately describe the open- and closed-time distributions within the burst. However, it is clear that inter-burst closed-time distributions are more complex, consisting of a "mixture of exponentials" (Colquhoun and Hawkes, 1995), and are not adequately described by the sum of a small number of exponentials (not shown). Therefore, we have not attempted to fit probability density functions (pdfs) with the sums of exponential components. The smooth lines superimposed on the experimental data in Figs. 5–7 are the predicted lifetime distributions of the models described below.

Open times show a single exponential distribution with mean ~1 ms both for WT and I154C single channel currents in the presence, or absence, of SUR1. Furthermore, this open time is not altered in the presence of ATP (Figs. 5, 7). After application of PIP_2, the open probability of WT+SUR1 channels increases considerably, but again, the open time is unaffected (Fig. 6). WT and WT[ΔC] channel closed-time distributions consist of at least two temporally
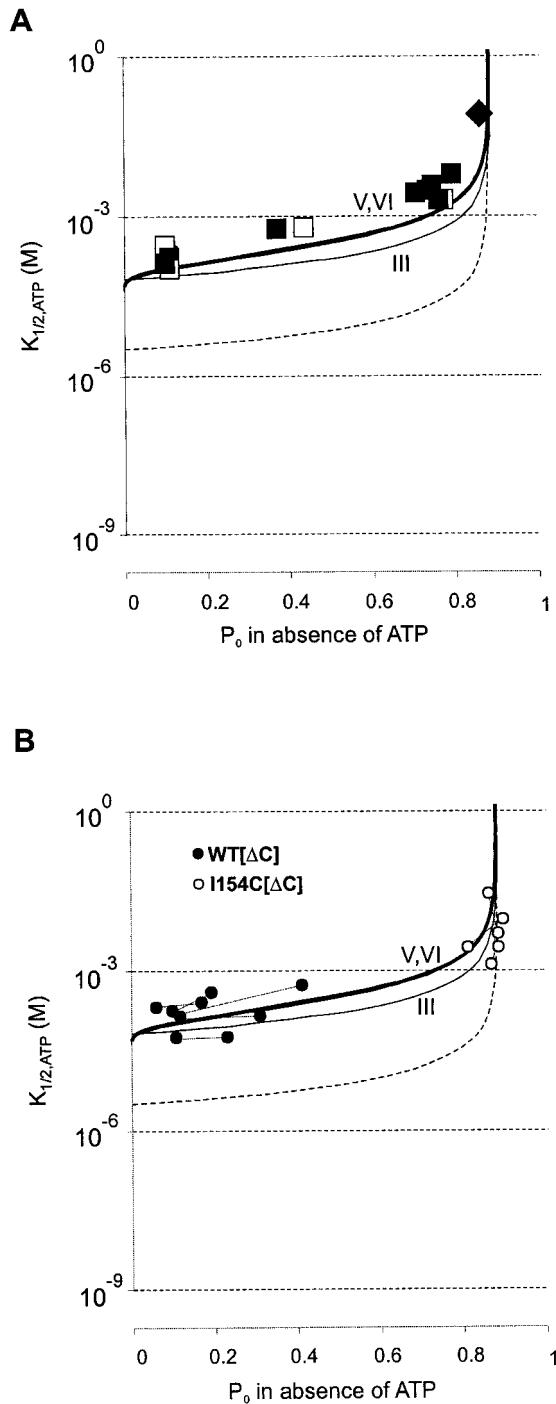
A

Table 2 $K_{1/2,ATP}$ and Po_{zero} values (estimated from noise analysis or single channels) for C-terminal truncated Kir6.2 channels expressed in the absence of SUR1

	$Po_{zero} \pm SE$	Mean $K_{1/2,ATP}$ (μM)
Ctrl	0.07 ± 0.01	122
Ctrl-[C166S, I154C]	0.73 ± 0.02	2,800
Ctrl-[C166S, M158C]	0.89 ± 0.02	>80,000
Ctrl*	0.11 ± 0.03	106
Ctrl-I167M*	0.45 ± 0.04	639
Ctrl-T171A*	0.43 ± 0.12	7,710
Ctrl-E179Q*	0.10 ± 0.01	296
Ctrl-C166S[†]	0.79 ± 0.02	2,820
Ctrl-C166T[†]	0.73 ± 0.04	3,800
Ctrl-C166A[†]	0.82 ± 0.03	6,100
Ctrl-C166M[†]	0.76 ± 0.04	4,200
Ctrl-C166F[†]	0.77 ± 0.03	5,300
Ctrl-C166L[†]	0.38 ± 0.05	584
Ctrl-C166V[†]	0.10 ± 0.04	136

Ctrl refers to Kir6.2[ΔC36] or Kir6.2[ΔC26] (Trapp et al., 1998) background, with other point mutations as indicated.
Values are from this study, in Tucker et al. (1998),* and in Trapp et al. (1998).[†]

B

FIGURE 4 $K_{1/2,ATP}$ versus Po_{zero} for Kir6.2 subunits expressed without SUR1 subunits (data summarized with errors in Table 2). (*A*) Large symbols represent different [ΔC] mutant constructs that demonstrate altered ATP-independent open probabilities (*squares:* data from Tucker et al., 1998, and Trapp et al., 1998; *diamond:* Kir6.2[ΔC36,C166S, M158C]). (*B*) Small symbols represent individual patches from WT[ΔC] (*closed symbols*) or I154C[ΔC] (*open symbols*), before and after exposure to PIP_2 (only peak responses are shown for clarity). Individual patches are connected by thin lines. Continuous lines in *A* and *B* represent predicted Po_{zero} versus $K_{1/2,ATP}$ relationships calculated from Models III, V (*heavy*), and VI in the absence of SUR1 (as indicated), together with the Model III relationship in the presence of SUR1 (*dashed*, taken from Fig. 2).

distinct components in the absence or presence of SUR1 (Figs. 5, 6). The shortest component (i.e., the intra-burst closures) would be reasonably well-fit with a single exponential with time constant ~0.5 ms, again with or without SUR1. Again, this intra-burst closed time is essentially independent of [ATP] (Fig. 5 *B*) and is unaffected by PIP_2 (Fig. 6). Consistently, the longer closed times appear as "mixtures of exponentials," i.e., single peaks in "Sigworth-Sine" plots, but spread over much wider time distributions than single exponentials, suggesting multiple overlapping exponential components (Colquhoun and Hawkes, 1995). These longer time components show a general trend of lengthening in the presence of ATP (Fig. 5), and shortening after PIP_2 application (Fig. 6).

We have also obtained single channel patches of high open-state stability I154C[ΔC] channels in the absence and presence of SUR1. Inspection of the single channel records indicates that in each case, channels are almost continuously bursting in the absence of ATP (Fig. 7). As with WT channels, open times are still monoexponential, and with the same time constant, ~1 ms. In the absence of ATP, closed-time distributions are dominated by a single short exponential of ~0.5 ms (Fig. 7). However, there is still a small "second" component in the closed-time distributions, in the presence and absence of SUR1. In both cases the amplitude of this component is increased, and the distribution shifted to longer times, in the presence of high [ATP].

In search of a unifying kinetic model of channel activity

Many models have been put forward to explain various aspects of the gating of K_{ATP} channels (e.g., Qin et al.,
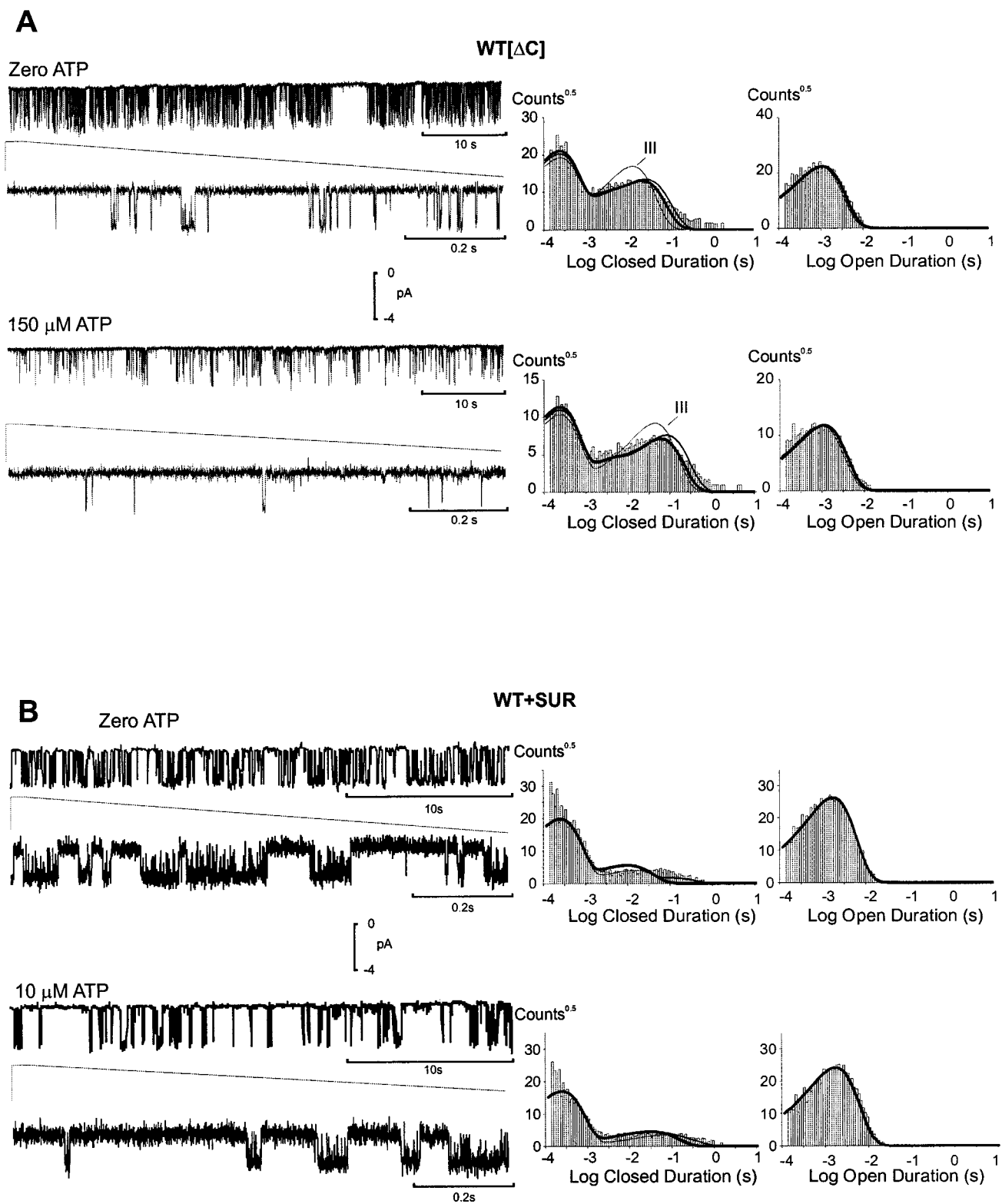
FIGURE 5 Representative single channel currents of WT[ΔC] alone (*A*) and WT + SUR1 (*B*) channels at −50 mV at different time scales, as indicated (*left*), together with Sigworth-Sine plots of closed- and open-lifetime distributions (*right*). Channels are shown in the absence and presence of [ATP]. The superimposed simulated probability density functions (pdfs) are predictions of kinetic Models III (*thin curve*), V (*heavy curve*), and VI (*medium curve*) described in the text.
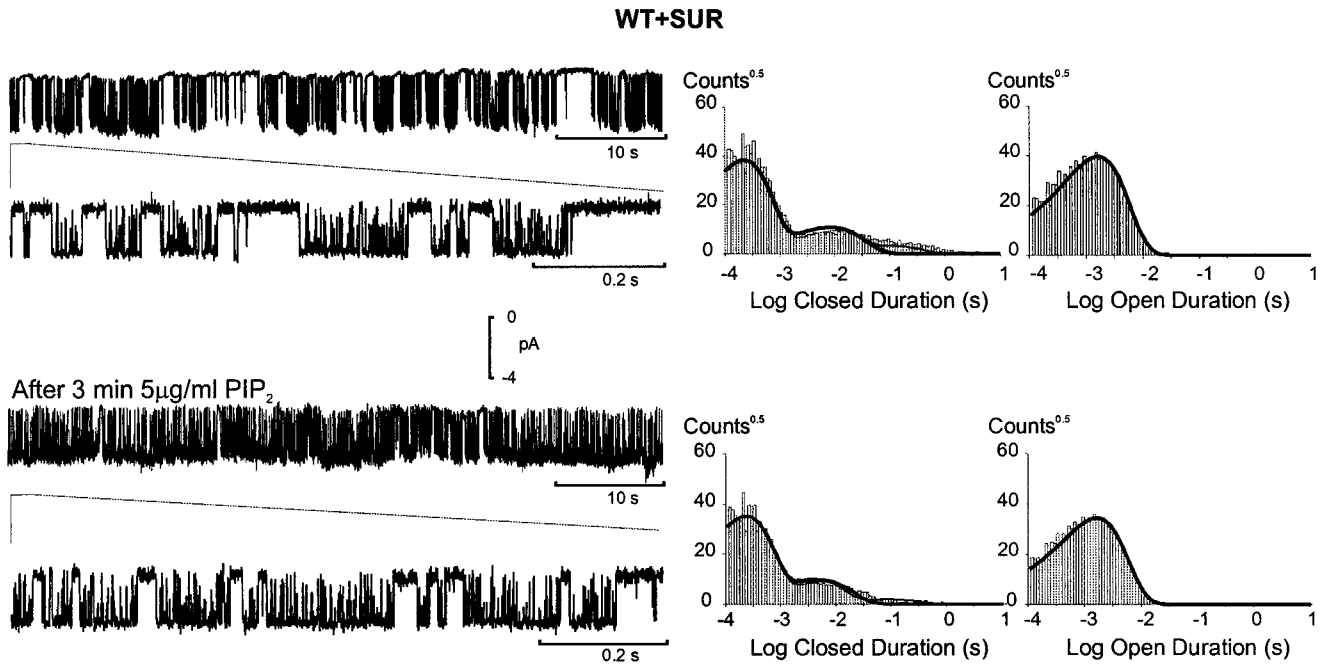
WT+SUR

FIGURE 6   Representative single channel currents of a WT + SUR1 channel before and after application of PIP_2, at -50 mV at different time scales, as indicated (*left*), together with Sigworth-Sine plots of closed- and open-lifetime distributions (*right*).The superimposed simulated probability density functions (pdfs) are predictions of kinetic Models III (*thin curve*), V (*heavy curve*), and VI (*medium curve*) described in the text.

1989; Nichols et al., 1991; Fan et al., 1990; Forestier et al., 1996; Alekseev et al., 1998; Trapp et al., 1998). None has thus far dealt with the interaction of PIP_2 with the channel, and many have not explicitly considered ATP binding, empirically describing only the apparent dependence of rate constants on [ATP]. The following features require explanation in any kinetic model of channel behavior: 1) endogenous K_{ATP} channels are typically inhibited with a $K_{1/2,ATP}$ of $\sim 10-40$ μM, and with best-fit Hill coefficients of between 1 and 2; 2) channel activity occurs in bursts, with closed times having multi-exponential distributions; 3) the brief closures are independent of ATP or PIP_2, but longer closures become longer still with increasing [ATP]; 4) channel open times are typically ATP-independent and have a single exponential distribution. Recent structure-function analyses raise another important consideration: channel activity is conferred by the Kir6.2 subunit (Shyng et al., 1997a; Tucker et al., 1997), but channel activity is significantly modified by the presence of SUR1 subunits (e.g., Tucker et al., 1997; Baukrowitz et al., 1998; John et al., 1998). Thus, reasonable adjustments should additionally allow any unified model to explain the kinetic behavior of channels in the presence and absence of SUR1. The additional information obtained from PIP_2 experiments further dictates that an appropriate model should also have specific steps that are dependent on, or modulated by, the binding of PIP_2.

The simplest model that could account for the four critical observations requires an ATP-independent closed state (C_f) in rapid equilibrium with the open state, and a longer closed state (C_0) to provide inter-burst closed states (e.g., Model I).

$$C_0 \leftrightarrow O \leftrightarrow C_f$$
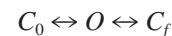
Model I

An indirect action of ATP could then be to shift the equilibrium between the C_0 and O-C_f states so as to prolong C_0. An additional C_1 state, accessed sequentially from C_0 (e.g., Model II, cf. Alekseev et al., 1998) would then allow two long closed states, as seems to be at least required by detailed analyses of wild-type (Kir6.2+SURx) channels (e.g., Nichols et al., 1991; Alekseev et al., 1998; Drain et al., 1998), and again, an undefined modulation of the equilibrium between C_1 and C_0 could prolong closed times in the presence of ATP.

$$C_1 \leftrightarrow C_0 \leftrightarrow O \leftrightarrow C_f$$
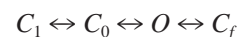
Model II

The lack of any evidence for more than one open state within the burst (see, e.g., Figs. 5–7; Drain et al., 1998; Alekseev et al., 1998) obviates the need to invoke more than one open state and argues that simple linear schemes (like Models I and II) might be appropriate models to explore.
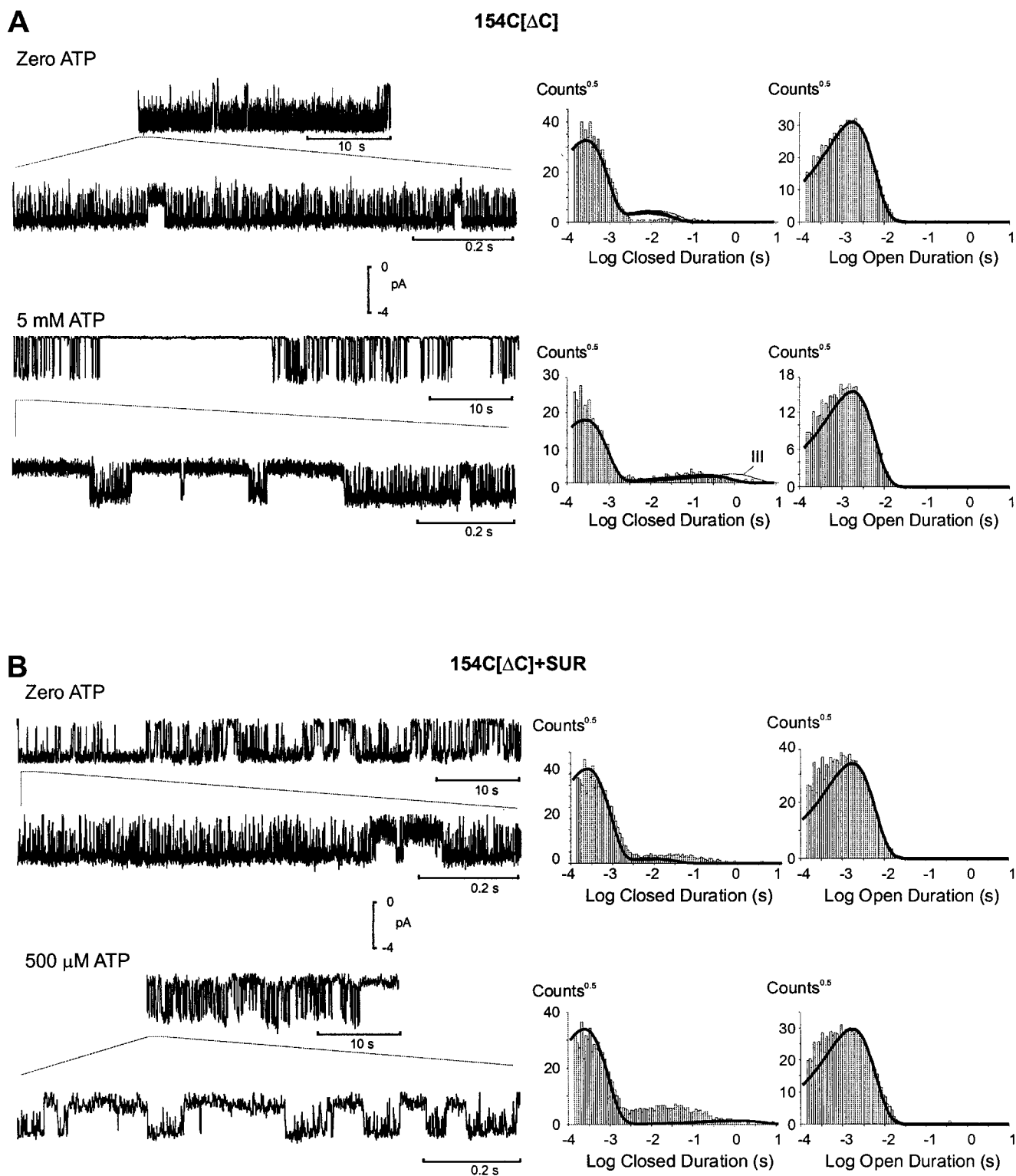
FIGURE 7   Representative single channel currents of I154C[ΔC] alone (A) and I154C[ΔC] + SUR1 (B) channels at −50 mV at different time scales, as indicated (left), together with Sigworth-Sine plots of closed- and open-lifetime distributions (right). Channels are shown in the absence and presence of [ATP]. The superimposed simulated probability density functions (pdfs) are predictions of kinetic Models III (thin curve), V (heavy curve), and VI (medium curve) described in the text.

Indirectly coupled models predict steady-state and kinetic data

The present data, which include modulation of channels by PIP_2 and the effect of multiple mutations, indicate a strict relationship between channel open probability and apparent ATP sensitivity. Without constraining ATP binding to a particular kinetic step, Models I and II do not predict any specific relationship between ATP sensitivity and Po_{zero}. The most reasonable explanation for the strong correlation of ATP sensitivity and open probability is that ATP must bind to, or its "action" be only felt by, a closed state, i.e., *ATP acts to stabilize a closed state*. This conclusion puts a critical constraint on understanding ATP inhibition, because it obviates a scenario in which ATP binds to the channel, then causes the channel to close. This constraint suggests exploring models that include a critical transition between the open state and a non-ATP-bound closed state (C_0), like the defined model (III) below:

$$C_1 \underset{k_{10}}{\overset{k_{01}*[ATP]}{\longleftrightarrow}} C_0 \underset{k_{CO}}{\overset{k_{OC}}{\longleftrightarrow}} O \underset{k_{OCf}}{\overset{k_{Cfo}}{\longleftrightarrow}} C_f$$
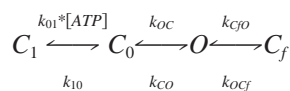
Model III

PIP_2, and numerous mutations (e.g., M2 mutations), "activate" channels by increasing Po_{zero} (Shyng et al., 1997a; Fan and Makielski, 1997; Shyng and Nichols, 1998; Tucker et al., 1998; Drain et al., 1998; Koster et al., 1999; Loussouarn et al., 2000). Po_{zero} is correlated in every case with change in ATP sensitivity (Figs. 2 and 4; see Note 2) implicating a mechanistic link between the two phenomena. Such a link is provided in Model III, because ATP binds to state C_0. Hence, if PIP_2, or a mutation in M2, shifts the equilibrium of the C_0-O transition (equilibrium constant $K_{CO} = k_{CO}/k_{OC}$) toward the open state (i.e., away from ATP-accessible states), then it both increases Po_{zero} and reduces apparent ATP sensitivity. In Figs. 2 and 4, the Po_{zero}-$K_{1/2,ATP}$ relationships predicted by this defined model are superimposed on experimental data (the rate constants are given in Table 3). We previously suggested that SUR1 acts to sensitize the Kir6.2 channels to ATP (Shyng et al., 1997b). Adjustments to Model III suggest that the steady-state behavior of channels expressed without SUR1 (Fig. 4) can be accounted for by assuming that the closed-state C_0 is energetically stabilized 20-fold, relative to the O and C_1 states, in the absence of SUR1. (i.e., SUR1 acts to destabilize this state). By stabilizing state C_0 in the absence of SUR1 (see Table 3), Model III predicts that the Po_{zero} and $K_{1/2,ATP}$ of WT[ΔC] channels shift from 0.69 and 15 μM, to 0.13, and 79 μM, in the presence and absence of SUR1, respectively, in good agreement with experimental data (Fig. 4). Moreover, as shown in Fig. 4, this single parameter adjustment shifts the whole Po_{zero}-$K_{1/2,ATP}$ curve to that observed for mutant channels expressed without SUR1 (Fig. 4).

Table 3 Rate constants used for simulations of WT channels by the different kinetic models

Model	k_{CO} (s^{-1})	k_{OC} (s^{-1})	k_{01} (μM^{-1} s^{-1})	k_{10} (s^{-1})	k_{01} (s^{-1})	k_{10} (s^{-1})
III	79	25*	500	1667*	—	—
V	130	13†	100†	667†	—	—
VI	140	14‡	150‡	664‡	8	13§

In all models, the intra-burst opening rate (k_{CfO}) and closing rates (k_{OCf}) were 4500 s^{-1} and 610 s^{-1}, respectively, giving a saturating $Po_{zero} = 0.88$. The above rate constants are for WT channels in the presence of SUR1. In the absence of SUR1: k_{OC} and k_{10} are increased 20-fold (i.e., to 500 s^{-1} and 33,330 s^{-1}, respectively), in model III(*); k_{OC} and k_{10} are increased, and k_{01} is decreased, 6-fold (i.e., to 78 s^{-1}, 4000 s^{-1}, and 16.7 μM-s^{-1}, respectively), in model V(†); k_{OC}, k_{10}, and k_{10} are increased, and k_{01} is decreased, 7-fold (i.e., to 98 s^{-1}, 4648 s^{-1}, 93 s^{-1}, and 21 μM-s^{-1}, respectively), in model VI (‡). In Fig. 6, k_{CO} is increased 2-fold in all models, after PIP_2 treatment.

Single channel lifetimes for Model III (and others below) were generated by matrix solution of the full kinetic schemes (see Methods), and are superimposed on measured lifetime distributions in Figs. 5–7. Appropriate rate constants were chosen within the constraints of steady-state equilibrium constants to simulate lifetime distributions seen in experiments (Figs. 5–7). Model III predicts a single, fast, open time and fast closed time, with a single, long, closed time in the absence of ATP. Only the long closed time is affected by ATP, becoming a longer "mixture of exponentials" with a single peak (e.g., Fig. 5 B). Model III predicts reasonable lifetime distributions for WT+SUR1 channels (Fig. 5 B) and the appropriate 20-fold increase of k_{OC} and k_{1O} (see Table 3) in the absence of SUR1 gives rise to considerably more long closed times in the absence of SUR1 (Fig. 5 A). By increasing k_{CO} 2-fold, PIP_2 is predicted to shorten the long closed-time distribution, in general agreement with observed lifetimes (Fig. 6).

For simulating lifetime distributions of I154C mutants with Model III (Fig. 7), k_{OC} was adjusted as shown in Table 4. Although Model III successfully predicts fast intra-burst closed- and open-time distributions, longer closed durations of both WT and I154C[ΔC] channels are not well accounted for, with or without SUR1, and this discrepancy is particularly severe in the absence of SUR1 (Fig. 7 A). Model III predicts single-exponential long closed distributions, at least in the absence of ATP (e.g., Figs. 5 A, 7 A), and not the "mixture of exponentials" that is observed.

Kinetic and steady-state constraints indicate a tetrameric model

In addition to problems with reproducing single channel lifetimes, Model III predicts a sigmoidal steady-state [ATP]-inhibition relationship, with Hill coefficient of 1, but the relationship is not well described by a Hill equation, even raised to a power. Steady-state ATP sensitivity is

Table 4 Rate constants used for simulations of I154C channels by the different kinetic models.

Model	k_{CO} sec^{-1}	k_{OC} sec^{-1}	k_{01} μM^{-1} sec^{-1}	k_{10} sec^{-1}	k_{01} sec^{-1}	k_{10} sec^{-1}
III	—	0.36	—	—	—	—
V	—	0.27	—	—	—	—
VI	—	0.25	—	—	—	—

In all models, the intra-burst opening rate (k_{CfO}) and closing rates (k_{OCf}) were 4500 s^{-1} and 610 s^{-1}, respectively, giving a saturating Po$_{zero}$ = 0.88. Only differences from wild-type are noted, i.e., rate constant k_{OC}, corresponding to 69-, 48-, and 56-fold increase in equilibrium constant K$_{CO}$. In the absence of SUR1: rate constants were altered using the same scaling as for WT channels.

shallow at low [ATP] (H ~1) and considerably steeper (approaching H = 4) at high [ATP] (Nichols et al., 1991, reviewed in Ashcroft and Gribble, 1998). Fig. 8 shows [ATP]-response relationships for WT+SUR1 channels, obtained by rapid application of multiple [ATP]. The non-sigmoidicity is clearly apparent, both for a single patch and when multiple patches are averaged (*inset*; see Note 3). This phenomenon, together with the complex kinetics of channel inhibition and activation after [ATP] "jumps," can be explained by models that assume multiple ATP molecules bind sequentially to stabilize closed states. Parameter fitting of such models (Nichols et al., 1991) indicated that a four-site model may be appropriate. Two or three sequential ATP binding steps do not provide adequate steepness at high [ATP], and given the 4-fold stoichiometry of the channel (Shyng and Nichols, 1997; Clement et al., 1997), two or three binding sites are unlikely. An appropriate model (e.g.,
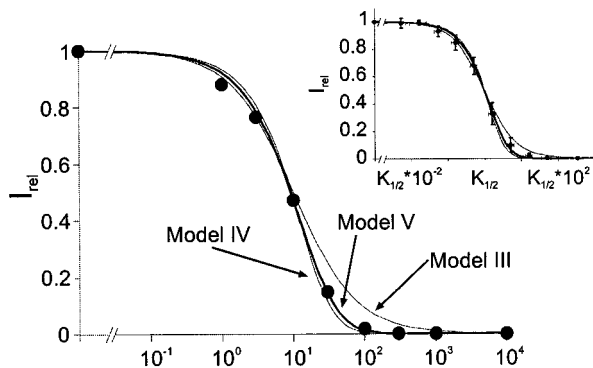

FIGURE 8 Relative current (Irel)-[ATP] relationship from an inside-out patch from cells expressing WT+SUR1 channels, and averaged data from multiple patches (*inset*). For the averaged data, individual relationships were "normalized" to the K$_{1/2,ATP}$ in order to avoid the shallowing effect of K$_{1/2,ATP}$ variability from patch to patch. The error bars indicate 95% confidence limits for the mean, (Student's *t*-distribution, assuming data are normally distributed). Note that the relationship is well described by Models III, IV, and V at low [ATP]. At higher [ATP], inhibition becomes a considerably "steeper" function of [ATP], and is not well described by the single ATP binding site model (III) but requires multiple ATP binding site models (IV and V). Model V lies within the 95% confidence limit for all data points, whereas Model III lies outside this limit for high [ATP]. Solid lines in both graphs are the predictions for Models III, IV, and V as indicated. Model IV assumes the same ATP-independent transitions as Model II, and independent binding of ATP at each subunit, with binding constant = 20 μM.

Model IV) can be generated as a linear extension of Model III:
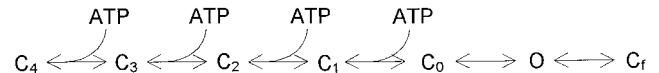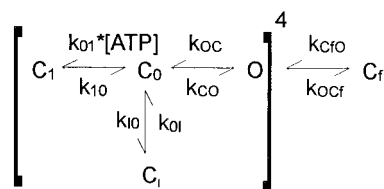

Model IV

This model reproduces appropriate steady-state [ATP]-inhibition relationships (Fig. 8), but does not give any better correlation of Po$_{zero}$ and K$_{1/2,ATP}$ than Model III (not shown). Moreover, it does not give any better prediction of the single channel kinetics of WT subunits with and without SUR1, because it reduces to Model III in the absence of ATP. Model IV still predicts a bi-exponential closed-time distribution, which is clearly inadequate to explain the observed distributions (e.g., Figs. 5–7). Multi-exponential long closed states with a linear model would require additional ATP-independent closed states between C$_0$ and O. We suggest instead a coupled model (V) involving four independent subunits, each of which can occupy only three distinct states. Model V assumes that each individual subunit can be in either the open (O) or closed state (C$_0$), and that a single ATP can bind to state C$_0$ to generate state C$_1$ for each subunit. The channel itself is open and conducting only when all four subunits are in the O state. Again, a separate fast closed state (C$_f$) is accessed from the open channel, giving rise to the "intra-burst" kinetics:
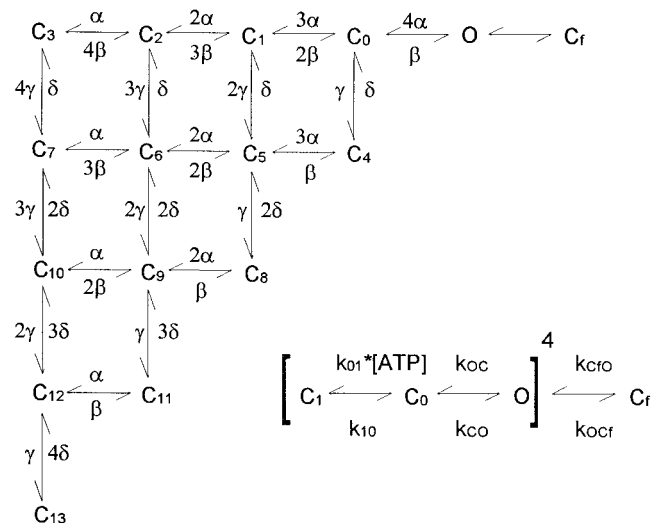
Model V

The model, drawn above in full on the left (to show the conformational changes of the whole channel), and on the right (to show the two transitions undergone by each independent subunit), is still governed only by the intra-burst rate constants (opening: k_{CfO} and closing: k_{OCf}) rate constants and by four other rate constants ($\alpha = k_{OC}$, $\beta = k_{CO}$, $\gamma = k_{01}*[ATP]$, $\delta = k_{10}$), but there are now a total of four overlapping inter-burst closed states in the absence of ATP (C_0–C_3), and 14 in the presence of ATP (C_0–C_{13}). This independent subunit model is analogous to the model proposed by Zagotta et al. (1994) to explain voltage-dependent gating of delayed rectifier K^+ channels. With a single set of parameters (Table 3), Model V not only reproduces steady-state [ATP]-response curves (Fig. 8) and $K_{1/2,ATP}$-Po_{zero} relationships (Figs. 2, 4), in the presence and absence of SUR1, but also predicts multi-exponential closed-time distributions that are generally closer to the experimentally observed distributions, particularly channels without SUR1 (Figs. 5 *A*, 7 *A*).

However, this model still fails to account for the very long closed states that are observed with low frequency in all channels and conditions (Figs. 5–7). Further complexity could be achieved by additional closed states. We suggest one final iteration (Model VI), which includes a longer "inactivated" closed state (C_I), accessible from C_0. Such a model still accounts for all of the major considerations, but provides additional long closed channel components in all pdfs, such as is apparent for wild-type channels (Fig. 5). Although this model is still controlled by only four equilibrium constants, the total number of transitions (61, with 36 total states) makes simulation cumbersome, and reaches the limit of what is justified by the data.

$$\left[C_1 \underset{k_{10}}{\overset{k_{01}*[ATP]}{\rightleftarrows}} C_0 \underset{k_{CO}}{\overset{k_{OC}}{\rightleftarrows}} O \underset{k_{OCf}}{\overset{k_{CfO}}{\rightleftarrows}} C_f \right]^4$$

$$C_0 \underset{k_{I0}}{\overset{k_{0I}}{\downarrow}} C_I$$

Model VI

DISCUSSION

The mechanism of ATP inhibition and PIP$_2$ activation

The K_{ATP} channel is unique among potassium channels in that activity depends strongly on cytoplasmic [ATP]. Understanding this inhibition is a central question, and recent studies have implicated the Kir6.2 subunit in controlling ATP-sensitivity (Shyng et al., 1997a; Tucker et al., 1997, 1998; Drain et al., 1998; John et al., 1998). These studies have not revealed the mechanism of ATP inhibition, although they have highlighted regions and residues (e.g., R50, K185, 334–337) that are involved. A majority of

mutations cause changes of ATP sensitivity ($K_{1/2,ATP}$) that are correlated with changes of channel open probability (Po_{zero}) (Tables 1 and 2; Figs. 2 and 4). The same relationship between $K_{1/2,ATP}$ and Po_{zero} is traversed, whether open probability is manipulated by PIP$_2$ treatment or by mutagenesis (Fig. 2, 4). This relationship can be explained by alterations in the equilibrium of a critical transition (K_{CO}) between the open (O) state and an ATP-accessible closed (C_0) state (Shyng et al., 1997a). Hence we conclude that ATP does not directly cause channel closure, rather *ATP stabilizes a closed state*. This conclusion was also reached by Shyng et al. (1997a) and Trapp et al. (1998), based on mutagenesis experiments, and can be inferred from the study of Alekseev et al. (1998) based on their analysis of single channel events. These effects of PIP$_2$ and M2 mutations (together with N-terminal truncations, Koster et al., 1999), are analogous to those of mutations in cyclic nucleotide-activated ion channels that alter the activating efficacy, but not the affinity, of cyclic nucleotides for these channels. For example, Gordon and Zagotta (1995) demonstrated that in chimeras between olfactory and rod cyclic nucleotide gated channels, cyclic nucleotide activating potency could vary over 3 orders of magnitude. This variable potency is a consequence of shifts in the equilibrium of the allosteric conformational change between closed and open states.

The role of SUR subunits in controlling channel kinetics

There exists a strong correlation between the $K_{1/2,ATP}$ and Po_{zero}, for channels expressed both with and without, SUR1 (Figs. 2, 4) but the relationship is different in the two cases. The anomaly of a higher $K_{1/2,ATP}$ and lower Po_{zero} for Kir6.2 expressed in the absence of SUR1 than in its presence has been noted previously (Tucker et al., 1997; Drain et al., 1998; John et al., 1998), but the mechanistic basis remains undetermined. The modeling in the present paper provides a potential explanation. The two Po_{zero}-$K_{1/2,ATP}$ relationships for the coexpressed (Fig. 2) and homomeric channels (Fig. 4) can be predicted by assuming that the presence of the SUR1 subunit destabilizes the ATP-unbound closed state (C_0 in each of the models). In the presence of SUR1, channels entering this state are more likely to transit to the ATP bound state (hence lower $K_{1/2,ATP}$ in control), and to the open state (hence higher Po_{zero}). In Model V, for instance, destabilization of state C_0 (w.r.t. states O and C_1) is the only adjustment necessary to reproduce the essential effects of SUR1 on both the $K_{1/2,ATP}$-Po_{zero} relationship and on single channel kinetics. Although there is presently no physical evidence to support or refute such a hypothetical effect of SUR1, it is conceptually simple to visualize the large SUR1 subunit somehow physically destabilizing the closed (C_0) state of Kir6.2.

It is quite clear from the present studies that the effects of PIP_2 on Kir6.2 channels coexpressed with SUR1 and on truncated Kir6.2 channels expressed alone are qualitatively similar, but quantitatively very different, as noted by Baukrowitz et al. (1998). In both cases the open-state stability increases, leading to increased open probability and reduced ATP sensitivity, but the I154C mutant experiments are necessary to conclusively demonstrate an increase in $K_{1/2,ATP}$ in channels expressed without SUR1. We have no ready explanation for the reduced effect of PIP_2 on channels expressed without SUR1. One obvious possibility is that PIP_2 binding to SUR1 occurs and that this interaction enhances the direct action of PIP_2 on Kir6.2. Clearly, the interaction between SUR1 and Kir6.2 is complex, and more intense biochemical analyses will be required to fully explain the kinetic effects of PIP_2.

Comparison with other mutagenic studies of Kir6.2

During the course of this study several groups examined the effects of Kir6.2 mutations on control of ATP sensitivity. Tucker et al. (1998) introduced random mutations throughout the N- and C-terminal regions of Kir6.2[ΔC26]. They demonstrated that mutations clustered between residues 39–51 in the N-terminus region, and between 166–185 at the end of the M2 segment and beginning of the C-terminal region could significantly decrease ATP sensitivity of channels expressed without SUR1. Of these mutations, R50G and K185Q reduced ATP sensitivity without changing the open probability in the absence of ATP (Po_{zero}), suggesting that these residues might actually reside within an ATP binding site. We have not examined such mutations in the present study, but their effects could be accounted for in the models by assuming changes of the ATP binding (k_{01}) or unbinding (k_{10}) rate constants. Tucker et al. (1998) isolated mutations C166S, I167M, and T171A, wherein decreased ATP sensitivity was associated with an increase in Po_{zero}. Trapp et al. (1998) examined ATP sensitivity and gating behavior of multiple mutations at position 166, also showing that altered ATP sensitivity of M2 mutants is in every case associated with a change in Po_{zero} (see Table 2, Fig. 4). Based on such results, Tucker et al. (1998) suggest that the intracellular end of M2 may contribute to an intracellular gate governing access to the pore. However, mutations that alter Po_{zero} and $K_{1/2,ATP}$ are clearly found throughout the M2 segment (Table 1). Rather than suggesting that a specific residue forms a "gate," it may be more reasonable to consider the whole of the M2 helix being the "gate," and the "gating process" (i.e., the C_0–O transition) involving either rotation or tilting of the helices, or both, as proposed for the gating of the bacterial KcsA channel (Perozo et al., 1998, see below).

Drain et al. (1998) also used a scanning mutagenesis strategy to examine the role of Kir6.2 in controlling ATP sensitivity. They identified two regions in the C-terminus that help determine ATP sensitivity. The first included residues 171–182 at the end of M2, mutations in this region being associated with increased Po_{zero} and further demonstrating that mutations of this region alter the stability of the open channel. The second region included residues 334–337 in the distal C-terminus. As with R50G and K185Q (Tucker et al., 1998; Koster et al., 1999), mutations in this region were not associated with altered Po_{zero}, consistent with an involvement in ATP binding, rather than control of a "gate." From these intense mutagenesis studies a picture emerges whereby ATP is likely to bind to residues in the cytoplasmic N- and C-termini. Very recently, Tanabe et al. (1999) have provided direct evidence for binding of 8-azido ATP to Kir6.2.

Comparison with other modeling studies

Several papers have attempted to model the complexities of the response of K_{ATP} channels to activating nucleotides and potassium channel openers (e.g., Fan et al., 1990; Forestier et al., 1996). However, only recently have attempts been made to model even ATP inhibition itself based on analysis of single channel events (Alekseev et al., 1997, 1998; Trapp et al., 1998; Drain et al., 1998). Qin and Noma (1988) developed the oil-gate chamber to examine the response to step changes of [ATP], in analogy to stepped voltage-clamp analysis of voltage-gated channels. In these experiments there is a pronounced lag in the response to step decrease of ATP (Qin et al., 1989), and this is probably explained by diffusion limitations resulting from recession of the membrane in the electrode tip. Taking such limitations into account requires complex analysis (Cannell and Nichols, 1991; Nichols et al., 1991). Baukrowitz et al. (1998) estimated apparent ATP on- and off-rates for inhibition using concentration jumps on inside-out macro-patches. They did not consider potential diffusion limitations, and interpreted their data with a very simplified two-state (active-inhibited) model. They concluded that PIP_2 acts to reduce the apparent on-rate of ATP but does not affect the off-rate. This is generally consistent with the predictions of the present models, in which a shift of the C_0-O equilibrium toward the O state would reduce accessibility of C_0 and reduce the macroscopic ATP inhibition rate. The activation rate would be unaffected because it is dependent on the intrinsic ATP off-rate. Unfortunately, attempts to use photolysis of caged ATP to circumvent the problem of diffusion limitations have thus far been fruitless (Nichols et al., 1990), but further efforts are warranted.

In the first paper to examine K_{ATP} channel activity, Noma (1983) estimated the [ATP]-inhibition response relationship of cardiac channels. He concluded, based on the steepness of this relationship, that more than one ATP molecule should be involved in channel inhibition. Since that time, other studies have consistently shown that ATP sensitivity

is best fit by a Hill coefficient of between 1 and 2 (see e.g., Ashcroft, 1988; Nichols and Lederer, 1991; Ashcroft and Gribble, 1998). Nichols et al. (1991) considered the steepness of the relationship explicitly, and as shown here for recombinant WT+SUR1 channels (Fig. 8), the relationship is not adequately explained by a simple Hill equation, even with a coefficient greater than 1. The linear model of Nichols et al. (1991) predicts a steady-state [ATP]-response relationship in which the limiting slope (Hill coefficient) approaches 1 at low [ATP], but approaches 4 at high [ATP]. A similar prediction arises from the present linear four-site model (IV) and the concerted models (V, VI). As shown in Fig. 8, these models predict the measured ATP sensitivity of Kir6.2+SUR1 channels better than single-site models (e.g., Model III).

Detailed analysis of *Shaker* Kv channel gating by Zagotta et al. (1994) suggests that independent gating motions of each of the four channel subunits may be required for the channel to conduct. The parallel between these models and the present models (V, VI) is intriguing in raising the possibility of common gating mechanisms. The cyclic nucleotide-gated (CNG) channels are also structurally within the potassium channel superfamily (Zagotta and Siegelbaum, 1996), although they are non-selective and show only very weak voltage-dependence. Nevertheless, detailed kinetic analyses suggest gating schemes that are conceptually similar to the one we propose here (e.g., Karpen et al., 1988). Again, rapid transitions within a burst are cyclic nucleotide-independent and closed times between bursts are [ligand]-dependent (Matthews and Watanabe, 1987; Haynes and Yau, 1990; Taylor and Baylor, 1995; Karpen et al., 1988). Recent data suggest that ligand-independent opening of these channels can occur (Picones and Korenbrot, 1995; Tibbs et al., 1997) necessitating a model in which the channel can open from any liganded or unliganded state (Monod et al., 1965; Stryer, 1987). In the present study we have not considered such models (e.g., VII), because there is as yet no evidence for K_{ATP} channel opening at saturating [ATP]; analyses of single channels (e.g., Figs. 5–7) do not indicate any dependence of open duration on [ATP].

$$C_0 \rightleftharpoons O \longrightarrow C_f$$
$$ATP \downarrow \quad ATP \downarrow$$
$$C_1 \rightleftharpoons O_1$$
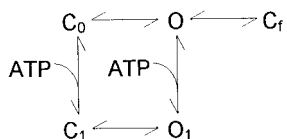
Model VII

At least for WT and other relatively low open-state stability mutants, the effects of manipulating the open-state stability on apparent ATP sensitivity requires that channels must enter a closed state before ATP can act. Very high open-state stability mutants, e.g., L164C, are so ATP-insensitive that we cannot practically measure ATP sensitivity over a full range, and so we cannot exclude the possibility that such channels may actually show ATP-insensitive openings.

The physical basis of the critical transition

It is clear that multiple mutations throughout the Kir6.2 subunit, including N-terminal truncations (Koster et al., 1999), regions in the C-terminal (Trapp et al., 1998; Tucker et al., 1998; Shyng and Nichols, 1998; Drain et al., 1998), and throughout the M2 segment (Fig. 3; Shyng et al., 1997a; Loussouarn et al., 2000), as well as PIP$_2$ (Shyng and Nichols, 1998; Baukrowitz et al., 1998), *all* control what may correspond kinetically to the same critical transition between the open state and the ATP-accessible closed state. The physical reality of such a transition is unknown, but disparate lines of evidence lead us to hypothesize the molecular basis. First, the crystal structure of the bacterial KcsA channel indicates that the four α-helical M2 domains line the inner vestibule of the channel, forming an inverted teepee, the four helices coming together at the point of the teepee to generate the internal entrance to the pore (Doyle et al., 1998). In lieu of a crystal structure of mammalian inward rectifiers, systematic cysteine scanning of the M2 domain in Kir6.2 reveals that this domain is also an α-helix with similar structure to the corresponding KcsA domain (Loussouarn et al., 2000). Moreover, EPR analysis of the M2 domain of KcsA reveals that the teepee-like structure "opens" during channel opening, moving the helices apart (Perozo et al., 1998). Motions of M2, making substituted cysteines less accessible, also occur during gating of Kir6.2 channels (Loussouarn et al., 2000). We hypothesize (Fig. 9), that the "critical-transition" corresponds to M2 helix motions, such that the open channel, stabilized by PIP$_2$, corresponds to the "opened" arrangement, and the closed channel, stabilized by ATP, corresponds to the "closed," teepee-like, arrangement. This scenario provides a ready explanation for the steric requirement of PIP$_2$ being in the membrane. It also provides an explanation why M2 mutations should have such profound effects on the equilibrium of the gating transition, because M2 itself is conceptually the "gate," and such mutations will control the stability of the critical open- and closed-conformations of the M2 helices.

NOTES

1. As in all kinetic analyses, the ability to identify discrete states is limited by the recording bandwidth. Missed events can cause added exponential components, or the elimination of exponential components (Blatz and Magleby, 1986), in lifetime distributions. Cursory analysis of corrections for missed events using the methods of Colquhoun and Hawkes (1995) for the two-state problem indicates that brief closed- and single open-times (Models III or V) would change by at most 2-fold (i.e., 0.3 log units), with longer closed-time components less affected. With an estimated dead-time of <80 μs, any additional components should appear with time constant <160 μs (Blatz and Magleby, 1986), well outside the long closed distri-
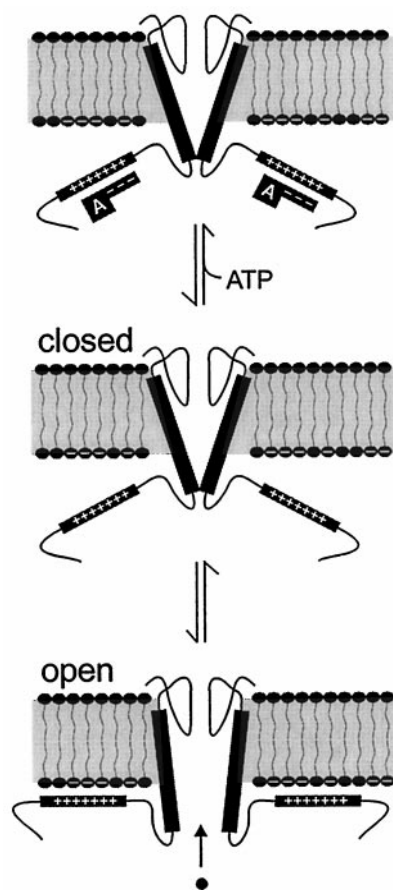
FIGURE 9 Cartoon to illustrate the hypothesized physical basis of the "critical transition." In the open state of the channel the transmembrane M2 helices that line the pore are opened relative to one another, and are stabilized in this position by association of the positively charged C-terminal domain to the membrane. The "critical transition" involves M2 helix-"collapse," closing off the pore at the cytoplasmic end. The C-terminal domain dissociates from the membrane lipid, and this closed state can then be stabilized by association with ATP.

butions we observe. As the overall multi-exponential nature of closed-time distributions will remain the same, we made no explicit corrections for missed events. Filtering at >5 kHz introduced rapid events resulting from open- or closed-channel noise and filtering at 1 kHz or less caused progressive prolongation of the apparent mean duration of the shortest open- and closed-times. Lifetime distributions were stable for filtering at 5 kHz and 3 kHz. Accordingly, detailed channel lifetime analyses were made after filtering at 3 or 4 kHz.

2. Some mutations affect ATP sensitivity without altering Po$_{zero}$ (e.g., R50G, K185Q, Tucker et al., 1998; replacement of residues 334–337, Drain et al., 1998). These may actually affect ATP binding, and so we have not discussed them here. However, the effects of such mutations could be accounted for in Models III–VI by assuming changes of the ATP binding (k$_{01}$) or unbinding (k$_{10}$) rate constants (Koster et al., 1999).

3. For multi-patch averaging, intrinsic variation of ATP sensitivity after patch isolation (Findlay and Faivre, 1991), which may well reflect differences in membrane PIP$_2$ levels, requires normalizing concentrations to the half-maximal effective concentration to avoid causing artefactual shallowing of the relationship.

REFERENCES

Aguilar-Bryan, L., C. G. Nichols, S. W. Wechsler, J. P. Clement IV, A. E. Boyd III, G. Gonzalez, H. Herrera Sosa, K. Nguy, J. Bryan, and D. A. Nelson. 1995. The β cell high affinity sulfonylurea receptor: a regulator of insulin secretion. *Science.* 268:423–426.

Alekseev, A. E., P. A. Brady, and A. Terzic. 1998. Ligand-insensitive state of cardiac ATP-sensitive K+ channels: Basis for channel opening. *J. Gen. Physiol.* 111:381–394.

Alekseev, A. E., M. E. Kennedy, B. Navarro, and A. Terzic. 1997. Burst kinetics of co-expressed Kir6.2/SUR1 clones: comparison of recombinant with native ATP-sensitive K+ channel behavior. *J. Membr. Biol.* 159:161–168.

Ashcroft, F. M. 1988. Adenosine 5′-triphosphate-sensitive potassium channels. *Annu. Rev. Neurosci.* 11:97–118.

Ashcroft, F. M., and F. M. Gribble. 1998. Correlating structure and function in ATP-sensitive K$^+$ channels. *Trends Neurosci.* 21:288–294.

Baukrowitz, T., U. Schulte, D. Oliver, S. Herlitze, T. Krauter, S. J. Tucker, J. P. Ruppersberg, and B. Fakler. 1998. PIP$_2$ and PIP as determinants for ATP inhibition of K-ATP channels. *Science.* 282:1141–1144.

Blatz, A. L., and K. L. Magleby. 1986. Correcting single channel data for missed events. *Biophys. J.* 49:967–980.

Cannell, M. B., and C. G. Nichols. 1991. The effects of pipette geometry on the time course of solution change in patch clamp experiments. *Biophys. J.* 60:1156–1163.

Clement, J. P. IV, K. Kunjilwar, G. Gonzalez, M. Schwanstecher, U. Panten, L. Aguilar-Bryan, and J. Bryan. 1997. Association and stoichiometry of K$_{ATP}$ channel subunits. *Neuron.* 18:827–838.

Colquhoun, D., and A. G. Hawkes. 1977. Relaxation and fluctuations of membrane currents that flow through drug-operated channels. *Proc. R. Soc. Lond. Ser. B.* 199:231–262.

Colquhoun, D., and A. G. Hawkes. 1981. On the stochastic properties of single ion channels. *Proc. R. Soc. Lond. Ser. B.* 211:205–235.

Colquhoun, D., and A. G. Hawkes. 1995. The principles of the stochastic interpretation of ion-channel mechanisms. *In* Single-Channel Recording. B. Sakmann and E. Neher, editors. Plenum Press, New York. 397–482.

Doyle, D. A., J. M. Cabral, R. A. Pfuetzner, A. Kuo, J. M. Gulbis, S. L. Cohen, B. T. Chait, and R. MacKinnon. 1998. The structure of the potassium channel: molecular basis of K$^+$ conduction and selectivity. *Science.* 280:69–77.

Drain, P., L. H. Li, and J. Wang. 1998. K-ATP channel inhibition by ATP requires distinct functional domains of the cytoplasmic C-terminus of the pore-forming subunit. *Proc. Natl. Acad. Sci. USA.* 95:13953–13958.

Fan, Z., and J. C. Makielski. 1997. Anionic phospholipids activate ATP-sensitive potassium channels. *J. Biol. Chem.* 272:5388–5395.

Fan, Z., K. Nakayama, and M. Hiraoka. 1990. Multiple actions of pinacidil on adenosine triphosphate-sensitive potassium channels in guinea-pig ventricular myocytes. *J. Physiol.* 430:273–295.

Findley, I., and J. F. Faivre. 1991. ATP sensitive K channels in heart muscle. Spare channels. *FEBS Lett.* 279:95–97.

Forestier, C., J. Pierrard, and M. Vivaudou. 1996. Mechanism of action of K channel openers on skeletal muscle K$_{ATP}$ channels. Interactions with nucleotides and protons. *J. Gen. Physiol.* 107:489–502.

Gordon, S. E., and W. N. Zagotta. 1995. Localization of regions affecting an allosteric transition in cyclic nucleotide-activated channels. *Neuron.* 14:857–864.

Gribble, F. M., S. J. Tucker, and F. M. Ashcroft. 1997. The essential role of the Walker A motifs of SUR1 in K-ATP channel activation by Mg-ADP and diazoxide. *EMBO J.* 16:1145–1152.

Haynes, L. W., and K.-W. Yau. 1990. Single-channel measurement from the cyclic GMP-activated conductance of catfish retinal rods. *J. Physiol.* 429:451–481.

Hilgemann, D. W., and R. Ball. 1996. Regulation of cardiac Na+,Ca2+ exchange and K_{ATP} potassium channels by PIP_2. *Science.* 273:956–959.

Huang, C. L., S. Y. Feng, and D. W. Hilgemann. 1998. Direct activation of inward rectifier potassium channels by PIP_2 and its stabilization by G-beta-gamma. *Nature.* 391:803–806.

Inagaki, N., T. Gonoi, J. P. Clement IV, N. Namba, J. Inazawa, G. Gonzales, L. Aguilar-Bryan, S. Seino, and J. Bryan. 1995. Reconstitution of IK_{ATP}: an inward rectifier subunit plus the sulfonylurea receptor. *Science.* 270:1166–1170.

Inagaki, N., T. Gonoi, J. P. Clement IV, C. Z. Wang, L. Aguilar-Bryan, J. Bryan, and S. Seino. 1996. A family of sulfonylurea receptors determines the pharmacological properties of ATP-sensitive K^+ channels. *Neuron.* 16:1011–1017.

Inagaki, N., T. Gonoi, and S. Seino. 1997. Subunit stoichiometry of the pancreatic β-cell ATP-sensitive K^+ channel. *FEBS Lett.* 409:232–236.

John, S. A., J. R. Monck, J. N. Weiss, and B. Ribalet. 1998. The sulfonylurea receptor SUR1 regulates ATP-sensitive mouse Kir6.2 K^+ channels linked to green fluorescent protein in human embryonic kidney cells (HEK 293). *J. Physiol.* 510:333–345.

Karpen, J. W., A. L. Zimmerman, L. Stryer, and D. A. Baylor. 1988. Gating kinetics of the cyclic-GMP-activated channel of retinal rods: flash photolysis and voltage-jump studies. *Proc. Natl. Acad. Sci. USA.* 85:1287–1291.

Koster, J. C., Q. Sha, S.-L. Shyng, and C. G. Nichols. 1999. ATP inhibition of K_{ATP} channels: control of nucleotide sensitivity by the N-terminal domain of the Kir6.2 subunit. *J. Physiol.* 515:19–30.

Lederer, W. J., and C. G. Nichols. 1989. Nucleotide modulation of the activity of rat heart K_{ATP} channels in isolated membrane patches. *J. Physiol.* 419:193–211.

Loussouarn, G., E. N. Makhina, T. Rose, and C. G. Nichols. 2000. Structure and dynamics of the pore of inward rectifier K_{ATP} channels. *J. Biol. Chem.* 275:1137–1144.

Matthews, G., and S. Watanabe. 1987. Properties of ion channels closed by light and opened by guanosine 3′,5′-cyclic monophosphate in toad retinal rods. *J. Physiol.* 389:691–715.

Monod, J., J. Wyman, and J. P. Changeux. 1965. On the nature of allosteric transitions: a plausible model. *J. Mol. Biol.* 12:88–118.

Nichols, C. G., and W. J. Lederer. 1991. ATP-sensitive potassium channels in the cardiovascular system. *Am. J. Physiol. Heart Circ. Physiol.* 261:H1675–H1686.

Nichols, C. G., W. J. Lederer, and M. B. Cannell. 1991. The ATP-dependence of K_{ATP} channel kinetics in isolated membrane patches from rat ventricle. *Biophys. J.* 60:1164–1177.

Nichols, C. G., E. Niggli, and W. J. Lederer. 1990. Modulation of ATP-sensitive potassium channel activity by flash-photolysis of "caged-ATP" in rat heart cells. *Pflueg. Archiv. Eur. J. Physiol.* 415:510–512.

Nichols, C. G., S.-L. Shyng, A. Nestorowicz, B. Glaser, J. Clement IV, G. Gonzalez, L. Aguilar-Bryan, A. M. Permutt, and J. P. Bryan. 1996. Adenosine diphosphate as an intracellular regulator of insulin secretion. *Science.* 272:1785–1787.

Noma, A. 1983. ATP-regulated K^+ channels in cardiac muscle. *Nature.* 305:147–148.

Perozo, E., D. M. Cortes, and L. G. Cuello. 1998. Three-dimensional architecture and gating mechanism of a K^+ channel studied by EPR spectroscopy. *Nat. Struct. Biol.* 5:459–469.

Picones, A., and J. I. Korenbrot. 1995. Spontaneous, ligand-independent activity of the cGMP-gated ion channels in cone photoreceptors of fish. *J. Physiol.* 485:699–714.

Qin, D., and A. Noma. 1988. A new oil-gate concentration jump technique applied to inside-out patch-clamp recording. *Am. J. Physiol. Heart Circ. Physiol.* 255:H980–H984.

Qin, D., M. Takano, and A. Noma. 1989. Kinetics of ATP-sensitive K^+ channel revealed with oil-gate concentration jump method. *Am. J. Physiol. Heart Circ. Physiol.* 257:H1624–H1633.

Shyng, S.-L., T. Ferrigni, and C. G. Nichols. 1997a. Control of rectification and gating of cloned K_{ATP} channels by the Kir6.2 subunit. *J. Gen. Physiol.* 110:141–153.

Shyng, S.-L., T. Ferrigni, and C. G. Nichols. 1997b. Regulation of K_{ATP} channel activity by diazoxide and MgADP: distinct functions of the two nucleotide binding folds of the sulfonylurea receptor. *J. Gen. Physiol.* 110:643–654.

Shyng, S.-L., and C. G. Nichols. 1997. Octameric stoichiometry of the K_{ATP} channel complex. *J. Gen. Physiol.* 110:655–664.

Shyng, S.-L., and C. G. Nichols. 1998. Phosphatidyl inositol phosphates control of nucleotide-sensitivity of K_{ATP} channels. *Science.* 282:1138–1141.

Sigworth, F. J., and S. M. Sine. 1987. Data transformations for improved display and fitting of single-channel dwell time histograms. *Biophys. J.* 52:1047–1054.

Stryer, L. 1987. Visual transduction: design and recurring motifs. *Chem. Scr.* 27B:161–171.

Tanabe, K., S. J. Tucker, M. Matsuo, P. Proks, F. M. Ashcroft, S. Seino, T. Amachi, and K. Ueda. 1999. Direct photoaffinity labeling of the Kir6.2 subunit of the ATP-sensitive K^+ channel by 8-azido-ATP. *J. Biol. Chem.* 274:3931–3933.

Taylor, W. R., and D. A. Baylor. 1995. Conductance and kinetics of single cGMP-activated channels in salamander rod outer segments. *J. Physiol.* 483:567–582.

Tibbs, G. R., E. H. Goulding, and S. A. Siegelbaum. 1997. Allosteric activation and tuning of ligand efficacy in cyclic-nucleotide-gated channels. *Nature.* 386:612–615.

Trapp, S., P. Proks, S. J. Tucker, and F. M. Ashcroft. 1998. Molecular analysis of K_{ATP} channel gating and implications for channel inhibition by ATP. *J. Gen. Physiol.* 112:333–350.

Tucker, S. J., F. M. Gribble, P. Proks, S. Trapp, T. J. Ryder, T. Haug, F. Reimann, and F. M. Ashcroft. 1998. Molecular determinants of K-ATP channel inhibition by ATP. *EMBO J.* 17:3290–3296.

Tucker, S. J., F. M. Gribble, C. Zhao, S. Trapp, and F. M. Ashcroft. 1997. Truncation of Kir6.2 produces ATP-sensitive K^+ channels in the absence of the sulphonylurea receptor. *Nature.* 387:179–183.

Zagotta, W. N., T. Hoshi, and R. W. Aldrich. 1994. *Shaker* potassium channel gating. III: Evaluation of kinetic models for activation. *J. Gen. Physiol.* 103:321–362.

Zagotta, W. N., and S. A. Siegelbaum. 1996. Structure and function of cyclic nucleotide-gated channels. *Annu. Rev. Neurosci.* 19:235–263.